COBEM 99
XV Congresso Brasileiro de Engenharia Mecânica
15th Brazilian Congress of Mechanical Engineering
22 - 26 de Novembro de 1999 / November 22 - 26, 1999 Águas de Lindóia, São Paulo,

MAGNETIC ORIGIN FORCED VIBRATIONS CALCULATION IN A ELECTRIC MOTOR CONSIDERING DIFFERENT LOAD CONDITIONS

CARLOS G.C.NEVES[1,*], NELSON SADOWSKI[1,]**
1 grucad-eel-ctc-ufsc, c.p. 476, 88040-900, fax: 55.48.234-3790 –Florianópolis-SC-Brazil
e-mails: *guilherm@grucad.ufsc.br, **nelson@grucad.ufsc.br

NEWTON S.SOEIRO[2,3,†], SAMIR N.Y.GERGES[2,††]
2 lva/emc-ctc-ufsc, c.p. 476, 88040-900, fax: 55.48.234-3790 – Florianópolis-SC-Brazil
3 dem - ct - ufpa, 66000 - 00 - Belém - PA - Brazil
e-mails: † newton@mbox1.gva.ufsc.br, ††gerges@mbox1.gva.ufsc.br

Abstract. *In this paper a Finite Element model is used to calculate the magnetic origin forced vibrations of a squirrel cage induction motor in two different operating conditions. This model allows to calculate the windings and bars currents, the magnetic forces and motor structure dynamic response. The Finite Element method is employed to discretize the electromagnetic field equations and the β - method is used to discretize the time derivatives of the field and external circuit equations. The magnetic forces acting on the squirrel-cage induction motor stator are obtained by a method based on the Maxwell's Stress Tensor. From it, the harmonic composition of the magnetic forces is evaluated. The second step in this work consists in proceeding with the mechanical FEM to obtain the natural and forced response of the stator mechanical structure. The forced vibrations calculations are validated by measurements.*

Keywords: *Vibration, Magnetic forces, Maxwell's stress tensor, Finite element method, Squirrel-cage induction motor, Resonance.*

1. INTRODUCTION

In this paper Finite Element time step model is used to calculate the squirrel cage induction motor vibratory forced response in two different operating conditions: no load and full load. Therefore, the finite element electromagnetic model have to be solved twice. This model calculates the winding and bar currents and the magnetic forces acting on the induction motor stator teeth. The magnetic forces $F(t)$ are obtained by a method based on the Maxwell Stress Tensor.

From the mechanical point of view, the stator structural finite model must to represent the constraints of these two different situations in terms of boundary conditions, thus for the no load motor operation are considered free - free stator boundary conditions and for the full load motor operation are considered null displacements boundary conditions at motor fixation. The flow chart of "Fig. 1" summarizes the calculation procedures.

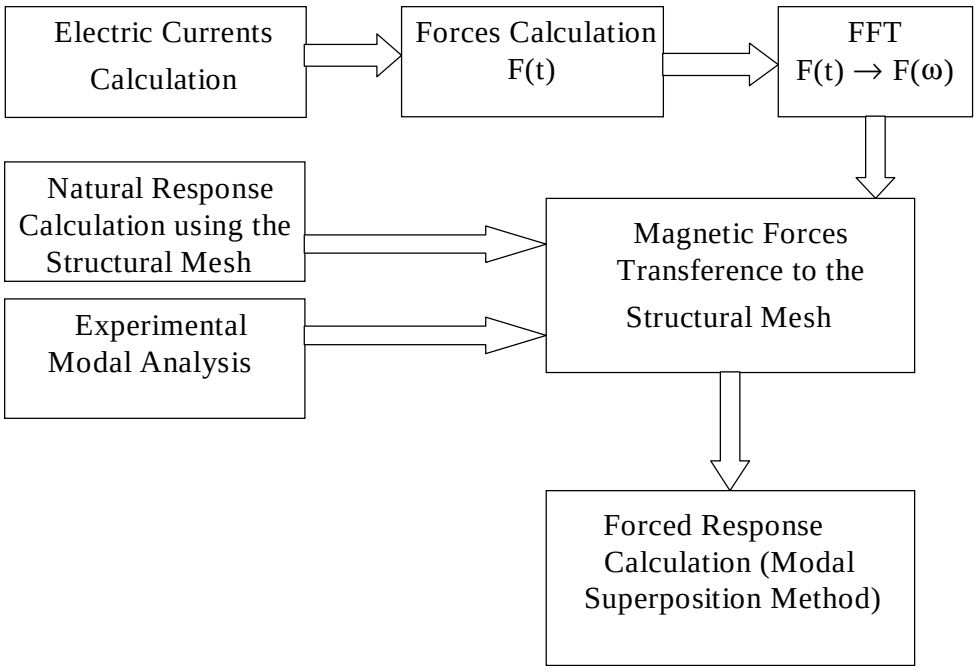

Figure 1 - Flow chart of the whole calculation.

2. ELECTROMAGNETIC SOLUTION

2.1 Electromagnetic model

Using the magnetic potential vector $\mathbf{A}$, the magnetic field in the machine can be written as:

$$\nabla \times {}^{1}\!/\!_{\mu} \times \nabla \times \mathbf{A} = \mathbf{J} - \sigma \, {}^{\partial \mathbf{A}}\!/\!_{\partial \mathbf{t}} \tag{1}$$

where μ is the magnetic permeability, **J** is the current density, σ is the electrical conductivity and ∇ is the nabla operator. The current density **J** in the machine coils is generally unknown, but may be related to the windings voltages $\mathbf{v}(t)$:

$$\mathbf{v}(t) = \mathbf{R}\mathbf{i}(t) + \mathbf{L} \, {}^{d\mathbf{i}(t)}\!/\!_{dt} + d \, {}^{\mathrm{N}\Phi(t)}\!/\!_{dt} \tag{2}$$

where $\mathbf{v}(t)$ is the input voltage vector, **R** is the windings voltages d. c. voltages, **L** is a inductance matrix which can contain the end windings inductances, $N\Phi(t)$ is the linkage matrix and $\mathbf{i}(t)$ is the windings current vector. The magnetic flux $\Phi(t)$ is related to the magnetic potential vector $\mathbf{A}(t)$.

Equation (1) is discretized by means of two dimensional Finite Element method, and time derivatives "Eqs. (1) and (2)" are discretized with the β - algorithm (Sadowski *et all.*, 1992). A large matrix system of equations in the obtained:

$$\left| \begin{array}{c|c} \beta\mathbf{M}(t) + {}^{1}\!/\!_{\Delta t}\,\mathbf{N} & -\beta\mathbf{P} \\ \hline {}^{1}\!/\!_{\Delta t}\,\lambda\mathbf{Q} & \beta\mathbf{R} + {}^{1}\!/\!_{\Delta t}\,\mathbf{L} \end{array} \right| \left| \begin{array}{c} \mathbf{A}(t) \\ \hline \mathbf{I_f}(t) \end{array} \right| =$$

$$= \left| \begin{array}{c|c} (\beta-1)\mathbf{M}(t-\Delta t) + {}^{1}\!/_{\Delta t}\,\mathbf{N} & (1-\beta)\mathbf{P} \\ \hline {}^{1}\!/_{\Delta t}\,\lambda\mathbf{Q} & (\beta-1)\mathbf{R} + {}^{1}\!/_{\Delta t}\,\mathbf{L} \end{array} \right| \left| \begin{array}{c} \mathbf{A}(t-\Delta t) \\ \hline \mathbf{I_f}(t-\Delta t) \end{array} \right| +$$

$$+ \left| \begin{array}{c} \mathbf{0} \\ \hline -\beta\mathbf{C}\mathbf{v}(t) \end{array} \right| + \left| \begin{array}{c} \mathbf{0} \\ \hline (\beta-1)\mathbf{C}\mathbf{v}(t-\Delta t) \end{array} \right| \qquad (3)$$

where **M** and **N** are respectively, magnetic permeability and electrical conductivity matrix. **P** and **Q** matrix relates field equations and electrical circuit equations. **0** is the null vector matrix, **v** is the input voltages related term. Δt é o passo de cálculo, λ is a factor which depends of the windings configuration (serial or paralel). The whole system (3) is solved step by step with respect to time, and the unknowns $\mathbf{A}(t)$e **i**(t) can be calculated.

2.2 Magnetic force calculation

The Maxwell Stress Tensor is used to calculate the magnetic forces, giving a force density $d\mathbf{f}/ds$ as follows (Sadowski *et all*, 1992).

$$\frac{d\mathbf{f}}{ds} = \frac{1}{\mu_0}\left[(\mathbf{n}\cdot\mathbf{B})\mathbf{B} - \frac{1}{2}B^2\mathbf{n}\right] \qquad (4)$$

where μ_0 is the permeability of the air, **n** is the vector normal to iron and **B** is the air side magnetic induction obtained with 2D Finite Element calculations. Figures 2(a) and 2(b) give the force distributions (indicated by the arrows) on a stator tooth for two different positions of rotor. In order to simplify the analysis, this force distribution is then concentrated on a point in the center of the inner surface of the tooth, for each rotor position. Rotation is taken into account by means of the Moving Band technique (Sadowski *et all*, 1992).

Figure 2 - Local force distribution on a tooth. (a) Rotor bar in front of a tooth. (b) Rotor bar dislocated of 10 degrees in relation to the tooth.

3. MODAL ANALYSIS

Modal analysis is used to extract the natural frequencies and mode shapes of a structure. Modal analysis is important as a precursor to any a dynamic analysis because knowledge of the structure's fundamental modes and frequencies can help to characterize its dynamic

response. Additionally, some forced response solution procedures, as the modal superposition method, requires the results of a modal analysis.

3.1 Numerical modal analysis

The natural frequencies and corresponding vibration modes can be obtained, using structural Finite Elements Method, by solving "Eq. (5)":

$$\mathbf{K}\mathbf{u}_r = \lambda \mathbf{M}\mathbf{u}_r \tag{5}$$

where λ is an eigenvalue; $\mathbf{u}_r$ is the corresponding eigenvector; **K** and **M** are, respectively, the rigidity and the mass matrices. Mechanical damping is neglected.

Figure 3 shows the radial stator mode shapes considering free - free boundary conditions. Figure 4 shows the main stator mode shapes considering null displacements boundary conditions at fixation of motor.

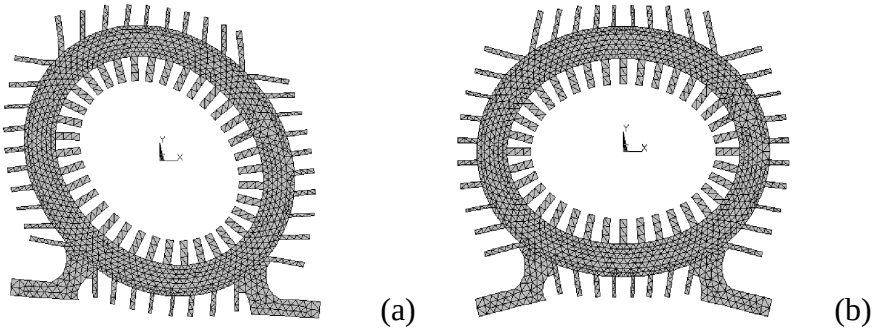

(a) (b)

Figure 3 - Modal analysis performed to determine the natural response considering free - free conditions. (a) 1309 Hz mode shape. (b) 1374 Hz mode shape.

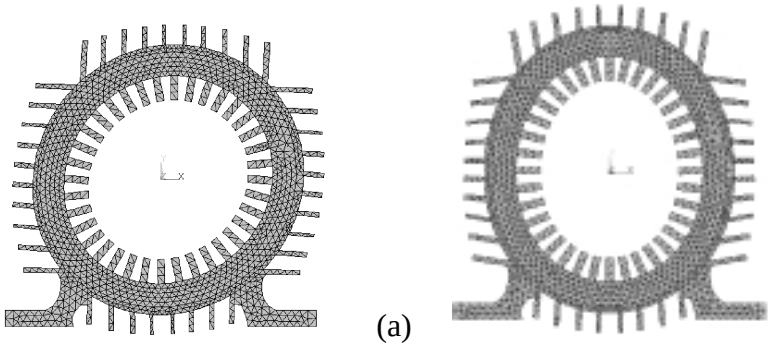

(a) (b)

Figure 4 - Modal analysis performed to determine the natural response considering null displacements boundary conditions. (a) 1283 Hz mode shape (b) 1348 Hz mode shape.

Comparing "Fig. 3(a)" with "Fig. 4(a)" one can notice that the movement restrictions change the natural frequencies and create a phase shift between the mode shapes. The same is observed comparing "Fig. 3(b)" with "Fig. 4(b)". This happens because the structure rigidity and mass change due to the base fixation.

3.2 Experimental Modal Analysis

The experimental Modal Analysis determines the structure modal model, i.e., its natural frequencies, modal damping and modal shapes. These quantities are obtained from a group of measured transfer functions. After measuring the frequency response functions, the modal parameters are extracted by curve fitting algorithms in time domain or in the frequency domain (Ewins, 1984). The force and acceleration signs were sampled simultaneously by a TEKTRONIX 2630 four channels FFT analyzer, with an anti-aliasing filter incorporated. Figure 5 shows, for the induction motor under analysis, the measured frequency response functions sum.

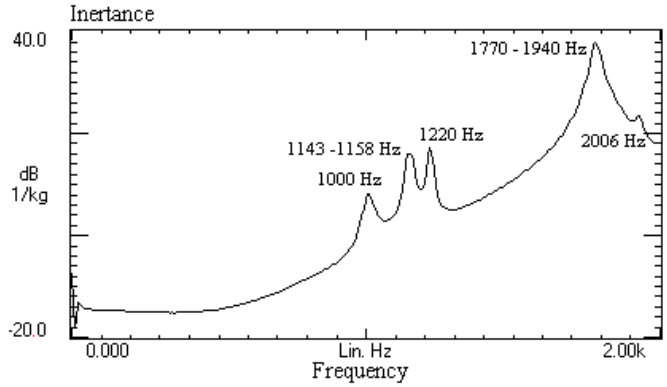

Figure 5 - Measured frequency response functions sum at free-free condition (100 Hz per division).

Table I shows a comparison among the natural frequency values obtained by FEM and them obtained by Modal Analysis, including the modal damping coefficients obtained by measurements.

TABLE I. Comparison among the Natural Frequency Values (Hz) Obtained by FEM and them obtained by Modal Analysis and Modal damping coefficients (%).

Mode	FEM (frequency)	Modal Analysis (frequency and damping)	Difference
1st	-	1002 (1.79%)	-
2nd	-	1143 (0.71%)	-
3rd	1309*	1158 (0.58%)	11.5
4th	1374*	1220 (0.56%)	11.2
5th	2306	1770 (0.84%)	23.2
6th	2313	1940 (0.84%)	16.1
7th	2528	2006 (0.46%)	20.6
			Average =16.5

- Radial Modes

Observing the values one can notice that the difference for the third and forth modes are 11.5 and 11.2, respectively, but increase for the higher modes.

4. MECHANICAL FORCED RESPONSE

4.1 Modal Superposition Method

Using the Modal Superposition Method the forced vibration response of a continuous structure (i. e. multiple degree of freedom system) to any force can be represented by the superposition of the various responses in their individual modes, considering each mode to respond as single degree freedom system. This method requires a natural response calculation prior to further solution steps.

The general equation of motion can be written as:

$$\mathbf{M}\frac{d^2}{dt^2}\mathbf{q}(t)+\mathbf{C}\frac{d}{dt}\mathbf{q}(t)+\mathbf{K}\mathbf{q}(t)=\mathbf{F}(t) \tag{6}$$

where $\mathbf{M}$, $\mathbf{C}$ and $\mathbf{K}$ are respectively the mass, damping and rigidity matrices, $\mathbf{q}(t)$ is the displacement vector and $\mathbf{F}(t)$ is the force vector. Using the next transformation matrix:

$$\mathbf{q}(t)=\mathbf{U}\,\mathbf{p}(t) \quad \text{or} \quad \mathbf{q}(t)=\mathbf{U}^T\,\mathbf{p}(t) \tag{7}$$

"eq. (7)" can be written in the modal coordinates space. In (7) $\mathbf{U}=\left\lfloor \mathbf{u}^1\ \mathbf{u}^2\cdots\mathbf{u}^N \right\rfloor$ is the eigenvectors matrix and $\mathbf{p}(t)$ is called modal displacement vector. By substituting (7) in (6) and after multiplying this result by $\mathbf{U}^T$, the transpose matrix of $\mathbf{U}$, the following expression is obtained:

$$\mathbf{m}\frac{d^2}{dt^2}\mathbf{p}(t)+\mathbf{c}\frac{d}{dt}\mathbf{p}(t)+\mathbf{k}\mathbf{p}(t)=\mathbf{f}(t) \tag{8}$$

where:

$$\mathbf{m}=\mathbf{U}^T\mathbf{M}\mathbf{U} \tag{9.a}$$

$$\mathbf{c}=\mathbf{U}^T\mathbf{C}\mathbf{U} \tag{9.b}$$

$$\mathbf{k}=\mathbf{U}^T\mathbf{K}\mathbf{U} \tag{9.c}$$

$$\mathbf{f}(t)=\mathbf{U}^T\mathbf{F}(t) \tag{9.d}$$

It can be verified that matrices $\mathbf{m}$ and $\mathbf{k}$ are diagonal because the eigenvectors are **M**-orthogonal. Matrix $\mathbf{c}$ is not generally diagonal but, in practice, only its diagonal terms, which can be obtained experimentally, are considered. Thus, the motion equation is a single degree of freedom equations set. Now, considering that the structure is excited by a forces set of the same frequency ω_h, but with many magnitudes and phases and assuming a response of the same form, "Eq. (8)" becomes, in the frequency domain (Javadi *et all.*,1995):

$$q_i=G_{ik}(\omega_h)F_k \tag{10}$$

where $G_{ik}(\omega_h)$ is a term of the so-called mechanical structure transfer matrix, which can be expressed as:

$$G_{ik}(\omega_h) = \sum_{r=1}^{N} \left\{ \frac{1}{m_r \omega_r^2 \left(1 - \frac{\omega_h^2}{\omega_r^2}\right) + jc_r \omega_h} u_r^i u_r^k \right\} \tag{11}$$

where N is the number of modes, u_r^i is the modal coordinate in the response position i, u_r^k is the modal coordinate in the excitation position k associated to mode r and m_r, ω_r and c_r are respectively the mass, natural frequency and damping coefficient of mode r.

From "Eq. (6)" the frequency response to each harmonic can be calculated taking into account the viscous damping of each mode. In this paper the damping constant hypothesis was adopted, this means: the average among the measured damping values was adopted.

4.2 Forced response calculation at no load

The calculated radial force acting on a tooth as a function of time and at no load condition is shown in "Fig. 6". The Fourier Analysis of this waveform gives a fundamental harmonic of 120 Hz. The frequency spectrum of the calculated force is given in "Fig. 7".

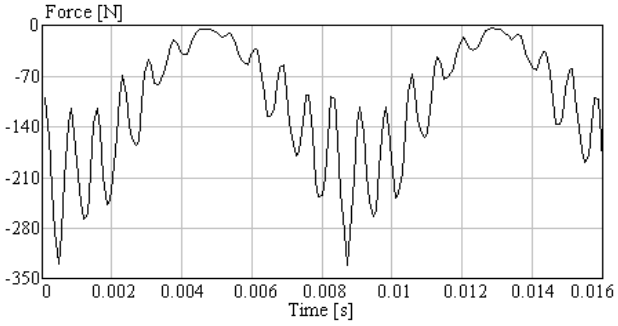

Figure 6 - Concentrated radial forces on a tooth as a function of time at no load condition.

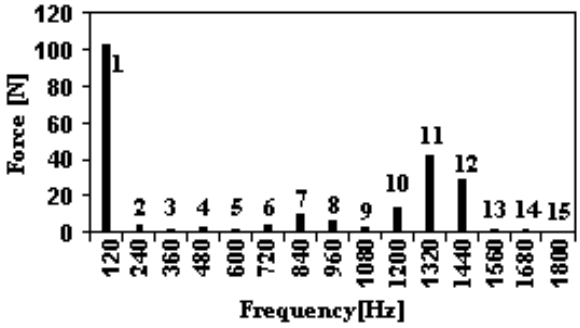

Figure 7 - Radial magnetic harmonic composition.

Figures 8 and 9 show, respectively, the calculated and measured accelerations as a function of the frequency, for the magnetic forces simulated at no load conditions. The ANSYS mechanical software was used to obtain these results.

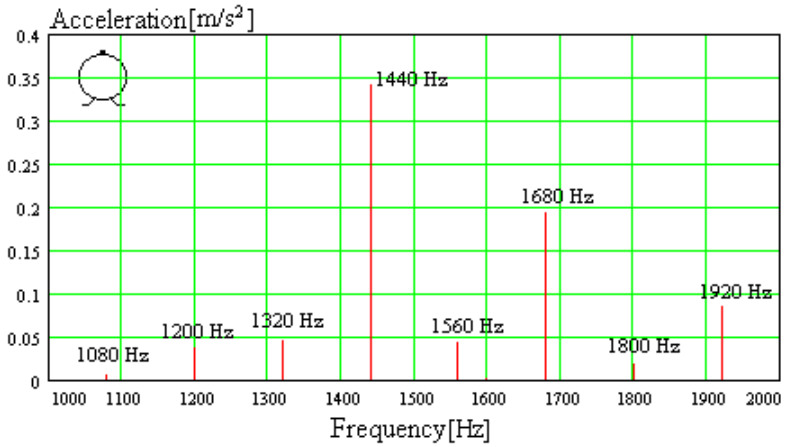

Figure 8. Calculated acceleration as a function of frequency. The icon shows the calculation point.

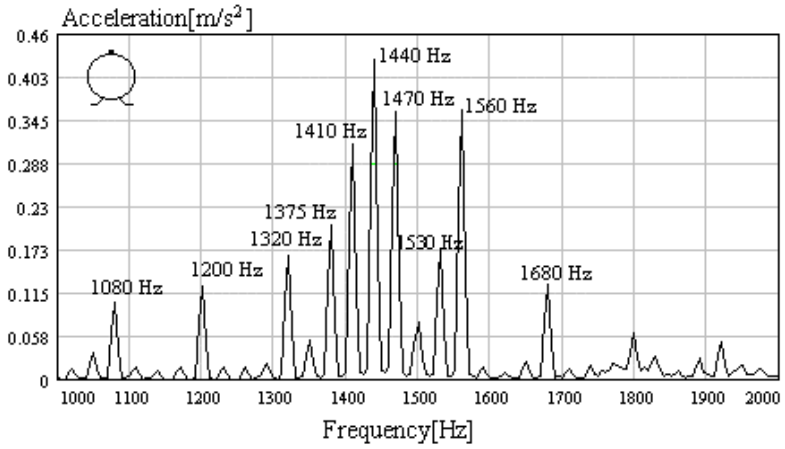

Figure 9. Measured acceleration as a function of frequency. The icon shows the measurement point.

Observing the calculated acceleration peak values one can notice that they present different values from the measured ones, mainly for those frequencies close to vibration mode shapes with significant longitudinal contribution, which are not foreseen by the numeric 2D finite elements modal model. This happens because the 2D model only provides the plane X-Y mode shapes; therefore the forced response just reflects the contribution of those modes shapes. An example is the 1560 Hz peak which has a very significant contribution of those modes. That fact can be verified mathematically through “Eq. (7)”. The absence of some important vibration modes in the mechanical model leads to a smaller $G(\omega_h)$ value and, in consequence, to a smaller acceleration peak at this frequency.

The 1410 Hz and 1470 Hz side bands that appear in the frequency of 1440 Hz can be explained by effects of rotor mechanical unbalance, once the difference of 30 Hz corresponds the rotation motor frequency of 1800 rpm.

4.3 Forced response calculation at full load

The calculated radial force acting on a tooth as a function of time and at full load condition is shown in “Fig. 10”. The Fourier Analysis of this waveform gives a fundamental harmonic of 120 Hz. The frequency spectrum of the calculated force is given in “Fig. 11”.

Figure 12 shows the calculated accelerations as a function of the frequency, for the magnetic forces simulated at full load condition.

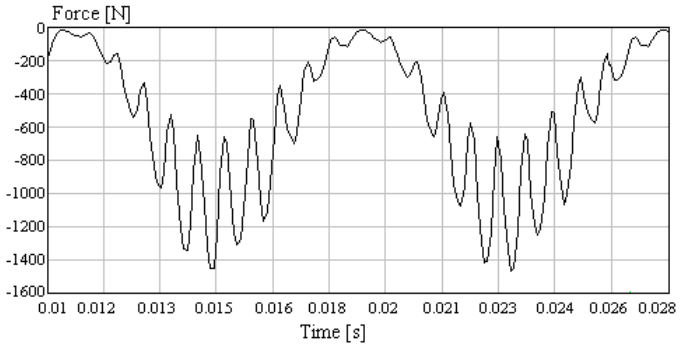

Figure 10 - Concentrated radial forces on a tooth as a function of time at full load condition**.**

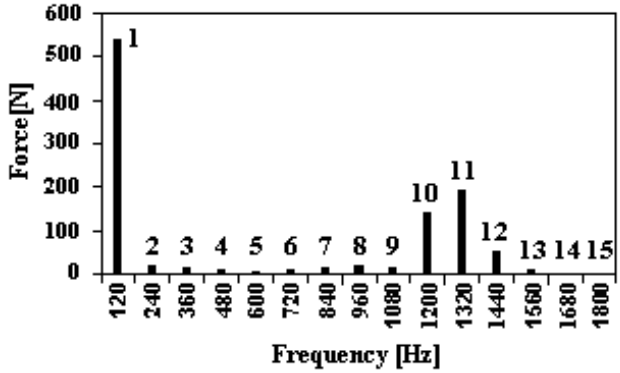

Figure 11 - Radial magnetic harmonic composition

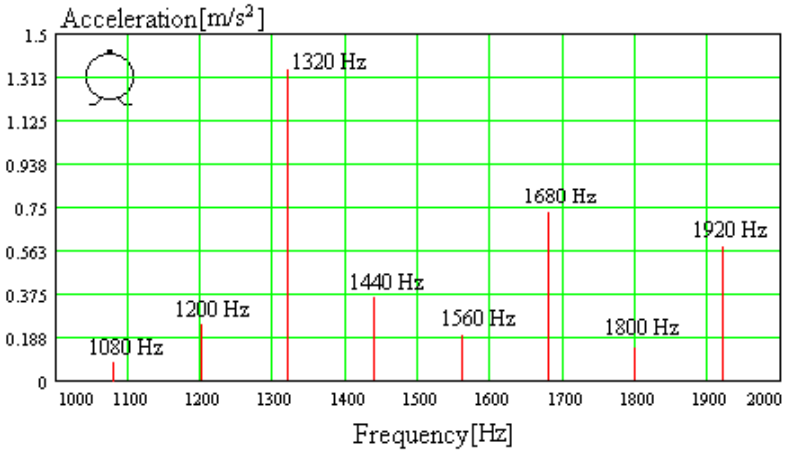

Figure 12 - Calculated acceleration as a function of frequency. The icon shows the calculation point.

Comparing “Fig. (8)” with “Fig. (12)” we observe that the accelerations spectrum is the same, since the spectrum of the magnetic forces is not modified. However, the accelerations magnitudes of “Fig. (12)” are much larger than the accelerations magnitudes of “Fig. (8)”, since magnetic forces values are very larger at full load operation than at no load operation.

Taking the stator structure forced deformations for 1440 Hz excitation frequency at no load condition (showed in “Fig. 13(a)”) and for the 1320 Hz excitation frequency at full load

condition (showed in “Fig. 13(b)”), one can conclude that at no load the 12th harmonic (1440 Hz) probably excites the 1374 Hz mode shape and at full load the 11th harmonic (1320 Hz) probably excites the 1348 Hz mode shape, because the forced deformations are similar to the mode shapes in both situations.

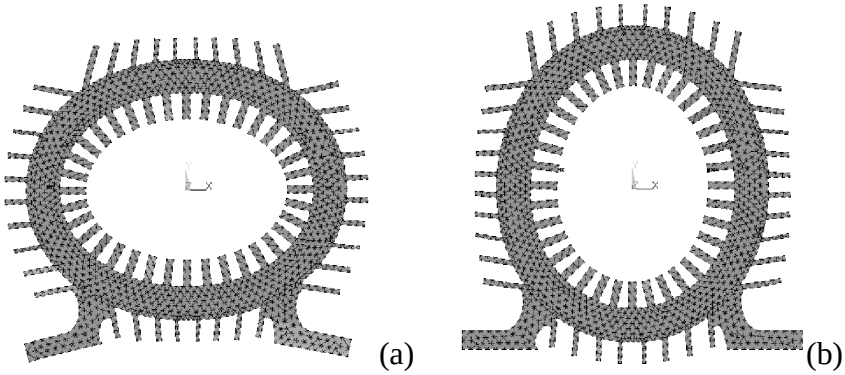

Figure 13. Deformations. (a) caused by the 12th harmonic (1440 Hz) of the magnetic forces at no load. (b) caused by the 11th harmonic (1320 Hz) of the magnetic forces at full load.

5. CONCLUSIONS

The local radial magnetic forces in the stator teeth is calculated by a method based on the Maxwell Stress Tensor for two load conditions: no load and full load. Mechanical Finite Element method is employed to obtain the natural response of the stator mechanical structure considering different boundary conditions related to the load condition. Mechanical Finite Element calculations give, finally, the deformations and accelerations for no load and for full load conditions. A good concordance between the calculated accelerations and the measured ones at no load condition is obtained. The operation conditions highly influence the vibrations magnitudes. The reasons for the main resonance peaks occurrence in both situations are explained.

REFERENCES

Ewins, D. J., Modal testing theory and pratice, 1995, Research Studies Press Ltd., England.

Javadi, H., Lefèvre, Y., Clenet, S., Lajoie-Mazenc, M., 1995, Electro-magneto-mechanical characterization of the vibration of magnetic origin of electrical machines, IEEE Trans. On Magn., Vol. 31, N. 3, pp. 1892-1895.

Sadowski, N., Lefèvre, Y., Lajoie-Mazenc, M., Cros, J., 1992, Finite element torque calculation in electrical machines while considering the movement, IEEE Trans. On Magn., Vol. 28, N. 2, pp. 1410-1413, March.

Sadowski, N.; Lefèvre, Y.; Lajoie-Mazenc, M., Bastos, J. P. A., 1992, Sur le calcul des forces magnétiques, Journal de physique III, France, pp. 859-870,.